



Intrinsic radiative lifetime derived via absorption cross section of one-dimensional excitons

Shaoqiang Chen¹, Masahiro Yoshita¹, Akira Ishikawa², Toshimitsu Mochizuki¹, Shun Maruyama¹, Hidefumi Akiyama¹, Yuhei Hayamizu³, Loren N. Pfeiffer⁴ & Ken W. West⁴

¹Institute for Solid State Physics, University of Tokyo, 5-1-5 Kashiwanoha, Kashiwa, Chiba 277-8581, Japan, ²Interdisciplinary Graduate School of Medical Science and Engineering, University of Yamanashi, Kofu, Yamanashi 400-8511, Japan, ³Department of Organic and Polymeric Materials, Tokyo Institute of Technology, 2-12-1 Ookayama, Meguro-ku, Tokyo 152-8500, Japan, ⁴School of Engineering and Applied Physics, Princeton University, Princeton, New Jersey 08544, USA.

SUBJECT AREAS:

NANOWIRES

SPECTROPHOTOMETRY

SEMICONDUCTOR LASERS

NANOPHOTONICS AND
PLASMONICS

Received
7 February 2013

Accepted
16 May 2013

Published
5 June 2013

Correspondence and requests for materials should be addressed to S.C. (shaoqiangchen@gmail.com)

Intrinsic radiative lifetime is an essential physical property of low-dimensional excitons that represents their optical transition rate and wavefunction, which directly measures the probability of finding an electron and a hole at the same position in an exciton. However, the conventional method that is used to determine this property via measuring the temperature-dependent photoluminescence (PL) decay time involves uncertainty due to various extrinsic contributions at high temperatures. Here, we propose an alternative method to derive the intrinsic radiative lifetime via temperature-independent measurement of the absorption cross section and transformation using Einstein's A-B-coefficient equations derived for low-dimensional excitons. We experimentally verified our approach for one-dimensional (1D) excitons in high-quality $14 \times 6 \text{ nm}^2$ quantum wires by comparing it to the conventional approach. Both independent evaluations showed good agreement with each other and with theoretical predictions. This approach opens a promising path to studying low-dimensional exciton physics.

Low-dimensional free excitons have optical transition rates that are concentrated within states having a center-of-mass wave vector $K \leq k_0 = n\omega_{ex}/c$, where $\hbar\omega_{ex}$ is the exciton energy, n is the refractive index, and c is the speed of light^{1–11}. Their radiative lifetime reflects the extent of center-of-mass motion and the tightly bound internal motion (wavefunction). Due to differences in the confinement dimensions, the radiative lifetime of 1D excitons becomes shorter than that of 0D excitons in molecules or dots and longer than that of 2D excitons. The 1D state is unique and essential in low-dimensional exciton physics because it is the lowest dimension that permits the motion of excitons.

The absolute values of the inverse radiative lifetime τ_K^{-1} of 1D excitons are scaled and characterized by the inverse intrinsic radiative lifetime τ_{1D}^{-1} or the averaged τ_K^{-1} over all K between 0 and k_0 , which is given by^{2–5}

$$\tau_{1D}^{-1} = \frac{\omega_{ex}^2}{3\epsilon_0\hbar c^2} |\varphi(0)|^2 \mu^2, \quad (1)$$

as schematically shown in Fig. 1a. Here, $\varphi(0)$ is the exciton internal wavefunction $\varphi(z)$ at an electron-hole relative distance $z = 0$; μ is the amplitude of the interband-transition dipole moment vector (μ_x, μ_y, μ_z); and ϵ_0 is the vacuum dielectric constant. The key equations, derivations, and related quantities of τ_{1D}^{-1} shown below are described in detail in the supplementary information. The intrinsic radiative lifetime τ_{1D} has been studied intensively in various 1D systems^{2–8}. In (In)GaAs, the value of τ_{1D} was theoretically calculated to be 150 ps² in a 10-nm diameter wire; τ_{1D} values in 2D wells and 0D dots have been reported to be shorter (by approximately 10 ps)^{1,12} and longer (by approximately 1 ns)¹³, respectively. For carbon nano-tubes, an *ab initio* calculation predicted a short τ_{1D} of 8–19 ps⁶, which is comparable to many experimental results^{7–10}.

However, τ_{1D} has been conventionally evaluated^{3–10} using the temperature-dependent PL decay time $\tau(T)$ of

thermalized 1D excitons, which is expressed as $\tau(T) = \tau_{1D} \sqrt{\frac{\pi k_B T}{4\Delta}}$ ($k_B T \gg \Delta = \frac{\hbar^2 k_0^2}{2M}$), where k_B is the Boltzmann constant, T is the temperature, and M is the exciton effective mass. We note here that the PL lifetime

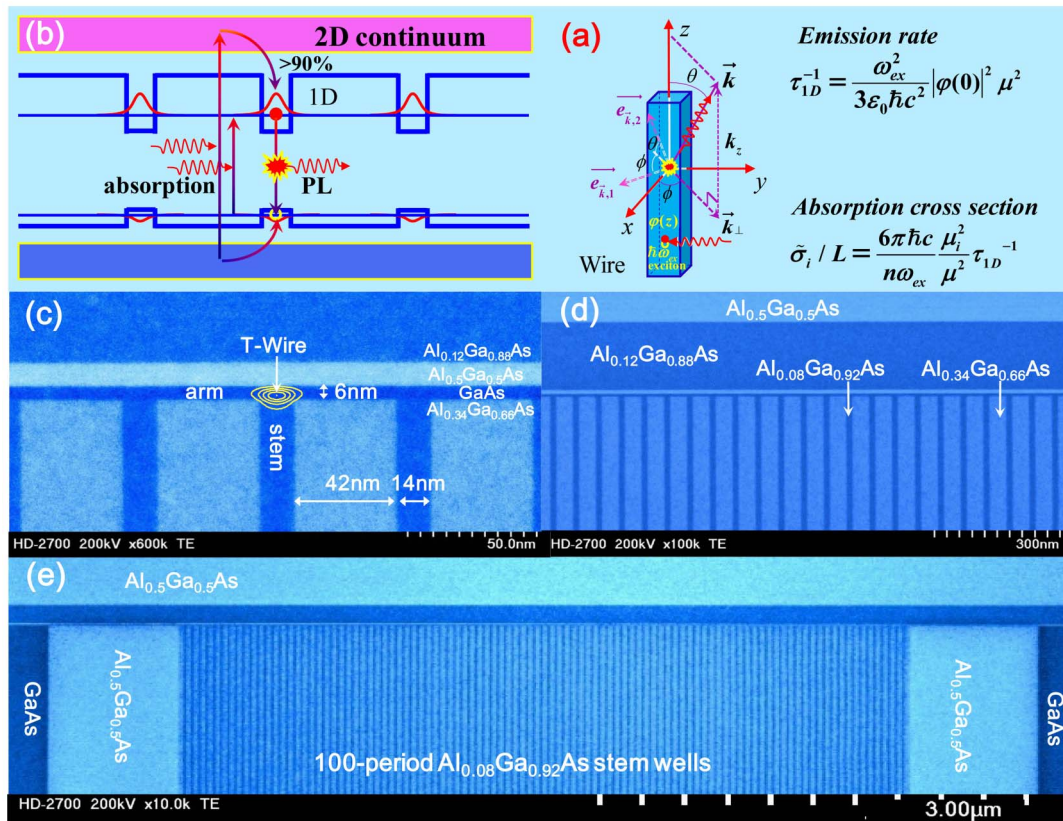


Figure 1 | Schematics of optical transition processes and cross-sectional transmission electron microscopy (TEM) images of 100-period T-shaped quantum wires. (a) An illustration of the optical emission and absorption processes of a 1D exciton in a quantum wire and the parameters used for calculations. (b) A schematic of optical pumping into 2D continuum states in the arm well, efficient carrier migration, and subsequent luminescence (PL) in T-wires. (c) A TEM image of T-wires. The thicknesses of the stem and arm wells are 14 and 6 nm, respectively. The stem wells and T-wires are uniformly separated by a barrier thickness of 42 nm. The T-wire states are formed at the intersection of the arm well and the stem wells as indicated by the contour curves of the T-wire wavefunction. (d, e) Magnified TEM images demonstrate the high uniformity of the T-wires and the precise replication of the stem wells and T-wires.

at elevated temperatures may be sensitive to extrinsic contributions, such as non-radiative decay, carrier migrations to/from adjacent regions, population migration to dark levels and/or higher levels, and band non-parabolicity. All of these factors induce uncertainty in the evaluation of τ_{1D} via PL lifetime. Hence, a different approach without relying on temperature dependence has been demanded.

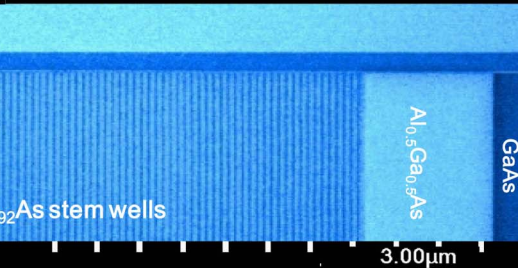
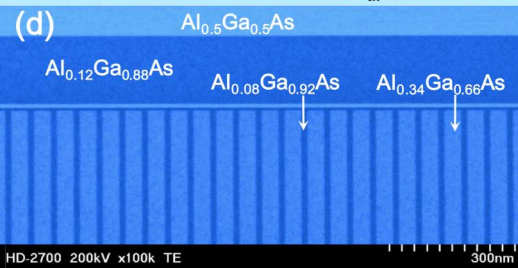
For alternative evaluation without measuring temperature dependence, we propose a new approach to derive the intrinsic lifetime τ_{1D} via the absorption cross section. Although the absorption probability of 1D excitons is extremely small due to the small volume of a quantum wire and is very difficult to measure, various techniques have so far been developed, such as external- and internal-light transmission measurements for waveguide-structured wires^{14–16}, combination of arbitrary-scale sensitive measurements and some absorption standards¹⁷, and direct transmission measurements for nanotube/nanowire solutions with controlled and characterized size and density distributions^{18,19}. If the integrated absorption cross section $\tilde{\sigma}_i/L$ of 1D excitons per unit length is measured by some means, it is then related to the inverse intrinsic lifetime τ_{1D}^{-1} of a 1D exciton as follows:

$$\tilde{\sigma}_i/L \equiv \int \sigma_i(\omega) d(\hbar\omega)/L = \frac{6\pi\hbar c \mu_i^2}{n\omega_{ex} \mu^2} \tau_{1D}^{-1} \quad (i = x, y, \text{ or } z), \quad (2)$$

where the subscript i ($i = x, y, \text{ or } z$) denotes the direction of incident light polarization. This equation is equivalent to the Einstein's A - B -coefficient relationship for 1D excitons. Indeed, assuming the random orientation of the wire with respect to the light field and using

$$\tau_{1D}^{-1} = \frac{\omega_{ex}^2}{3\epsilon_0 \hbar c^2} |\varphi(0)|^2 \mu^2$$

$$\tilde{\sigma}_i/L = \frac{6\pi\hbar c \mu_i^2}{n\omega_{ex} \mu^2} \tau_{1D}^{-1}$$



$\langle \mu_i^2 \rangle = \mu^2/3$, we obtain the angle-averaged expression $\langle \tilde{\sigma}_i \rangle/L = \frac{2\pi\hbar c}{n\omega_{ex}} \tau_{1D}^{-1}$ or, written in a more intuitively acceptable form, $B/L = 2 \frac{\pi c^2}{n^2 \omega_{ex} \hbar \omega_{ex}} A$ ($\tau_{1D}^{-1} = A$, $\langle \tilde{\sigma}_i \rangle = \frac{\hbar \omega_{ex}}{c/n} \hbar B$). Here, the factor of 2, $n^2 \omega_{ex}/\pi c^2$, and $\hbar \omega_{ex}$ are derived from spin degeneracy, the 2D photon density of states, and the photon energy at the exciton resonance, respectively. Note that the relationship for 1D excitons is different from the original, familiar Einstein A - B relationship for atomic dipole systems with a 3D photon density of states due to the low dimensionality (Fig. 1a).

Because such an approach has never been tested nor compared with the conventional approach, it is important to test both using an identical sample. To this end, we employed 100 identical non-doped $14 \times 6 \text{ nm}^2$ GaAs T-shaped quantum wires (T-wires)^{20,21} fabricated by cleaved-edged overgrowth and growth-interrupt annealing using molecular beam epitaxy. Cross-sectional transmission electron microscopy images (Fig. 1c–e) show that all T-shaped intersections of the 14-nm-thick stem wells on the (001) plane and the 6-nm-thick quantum well (arm well) on the (110) plane uniformly form 100 identical $14 \times 6 \text{ nm}^2$ T-wires with equal periods of 56 nm.

To evaluate the absorption cross section of 1D excitons or the absolute absorption probability at the 1D-exciton absorption peak with small uncertainty or errors, we use a reference or a standard of the 2D-continuum absorption plateau in a GaAs quantum well. Similarly to the quantum Hall resistance standard²² of a 2D electron gas providing the universal constants of $R_K = h/e^2$ or the

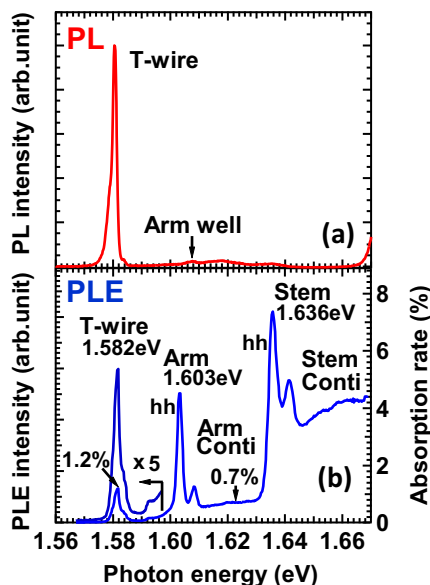


Figure 2 | Micro-PL and micro-PL excitation (PLE) spectra of the 100-period T-shaped quantum wires at 5 K. (a) shows the PL spectrum at an excitation energy of 1.696 eV, illustrating that the emission peak from the T-wires is very sharp and strong; in contrast, the peaks from the arm and stem wells are very weak, indicating that most of the photo-generated carriers flow into the wires rapidly within their lifetime. (b) shows the PLE spectrum of the T-wires at excitation energies from 1.550 eV to 1.696 eV. The energy levels of the T-wire structure are clearly demonstrated, such as the wire state (1.582 eV), wire continuum states (greater than 1.592 eV), arm state (1.603 eV), arm continuum states (greater than 1.620 eV), stem state (1.636 eV), and stem continuum states (greater than 1.660 eV). The right vertical axis measures the absorption rate of the T-wires calibrated by the continuum state of the arm well indicated by the arrow (0.7%). Arb. unit is an abbreviation of arbitrary unit.

fine-structure constant $\alpha_f = e^2/4\pi\epsilon_0\hbar c \approx 1/137$, the optical absorption probabilities of some 2D materials have recently been shown to be equal to universal constants^{17,23–25}. Indeed, the optical absorption probability of a single sheet of graphene is shown equal to $\pi\alpha_f$ ($\approx 2.3\%$)^{23,24} and that of the 2D-continuum absorption plateau in a GaAs quantum well is to $\zeta\pi\alpha_f/n$ ($\approx 0.7\%$)^{17,26}, where ζ is a correction factor (close to 1) that is only weakly dependent on structure and material^{17,25}.

Results

Figure 2 shows the micro-PL and micro-PL excitation (PLE) spectra of the samples at 5 K. The strong PL peak of the T-wires was detected at 1.581 eV (Fig. 2a). The Stokes shift (0.7 meV) of the ground state excitons in the T-wires is smaller than the PLE peak width of 2.4 meV, demonstrating the high quality of the T-wires (Fig. 2b). Even though the excitation light at 1.696 eV initially creates excitons in the arm well and stem wells, the PL from the T-wires is dominant in the PL spectrum. This result indicates that most (greater than 90%) of the carriers created in the arm well flow rapidly to adjacent T-wires (Fig. 1b), which supports our assumption that the PLE spectrum in the spectral region of the T-wires and the arm well is proportional to their absorption probability.

In the PLE spectrum, the sharp peaks at 1.603 and 1.636 eV are assigned to 2D exciton absorption in the arm and stem wells, respectively. The peak at 1.608 eV is due to the absorption of monolayer (ML) islands in the arm well. A flat plateau of the 2D continuum absorption of the arm well is clearly found in the region of 1.610–1.630 eV. The other resonances as the stem wells and the quantum wires are far from there. Thus, we may safely attribute the absorption

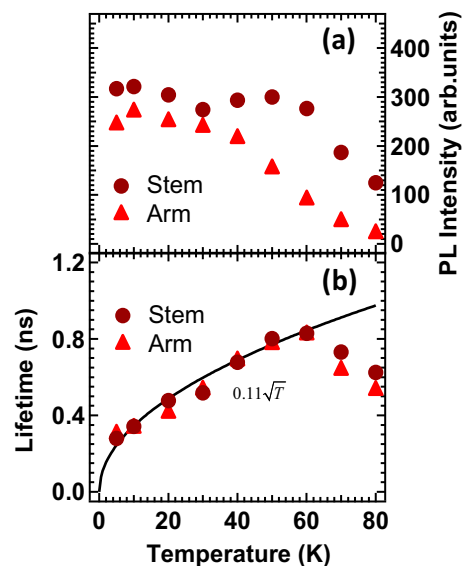


Figure 3 | Temperature-dependent time-resolved PL measurements of the 100-period T-shaped quantum wires. (a) Temperature dependence of the integrated PL intensities obtained using stem continuum excitation and arm continuum excitation. The intensities decrease significantly at temperatures greater than 60 K, where the non-radiative processes dominate. (b) Radiative lifetimes of excitons in T-wires measured at various temperatures from 5 K to 80 K. The results are well fitted by $\tau(T) = 0.11\sqrt{T}$, which is indicated by the solid line. Arb. units is an abbreviation of arbitrary units.

strength at 1.620 eV solely to the arm-well continuum absorption. We utilized the 2D-continuum absorption as a standard of absorption strength equal to $\zeta\pi\alpha_f/n$. After evaluating the correction factor ζ for the present case¹⁷, we obtained a value of 0.7% for the absolute absorption probability of the plateau, thus calibrating the PLE spectrum to the absorption spectrum as indicated in the vertical scale of Fig. 2b. Hence, the peak absorption rate of the 1D exciton peak at 1.582 eV is read as 1.2%. Because the T-wires are arrayed precisely every 56 nm, the peak absorption cross section per length σ/L becomes 0.67 nm, resulting in the energy-integrated absorption cross section per unit length $\tilde{\sigma}/L = 2.43$ meV nm. Finally, by using equation (2) and including the estimated uncertainty of $\pm 20\%$, we obtain $\tau_{1D} = 110 \pm 20$ ps for the 1D excitons in the T-wires (see supplementary information).

We separately measured the temperature-dependent PL decay time of 1D excitons in the same sample and characterized the intrinsic radiative lifetime via the conventional method^{3–5}. Figure 3 is a plot of the measured values of the integrated PL intensities and exciton PL lifetimes $\tau(T)$ at various temperatures T . Whereas the PL lifetime becomes longer with increasing temperature below 60 K, it decreases rapidly at temperatures greater than 60 K. The integrated PL intensity also decreases significantly at temperatures greater than 60 K, indicating that the decreased lifetime is most likely due to enhanced non-radiative decay or carrier escape from the T-wires. Thus, we compared the observed decay times at temperatures less than 60 K with the theoretically predicted \sqrt{T} -temperature dependence for the radiative lifetime of thermalized 1D excitons and obtained the best fit to $\tau(T) = 0.11\sqrt{T}$ ns. Using the measured value of $\tau(T) = 0.11\sqrt{T}$ ns and the estimated exciton mass of $M = 0.2 m_0$ ($\Delta = 0.133$ meV) for the motion along the T-wires near $K = 0$, we obtained $\tau_{1D} = 150$ ps. Due to possible complexities at high temperatures, this approach gives a large uncertainty of 0.16–2, or $\tau_{1D} = 25$ –300 ps (see supplementary information). Despite the high uncertainty, the value $\tau_{1D} = 150$ ps (25–300 ps), which was estimated via the temperature-dependent PL decay time, shows good agreement



with the value $\tau_{1D} = 110 \pm 20$ ps obtained via the absorption cross section. The reason for the low uncertainty in the new method is that it relies mostly on the basic physics of Einstein's relationship and the 2D absorption standard.

Discussion

The intrinsic radiative lifetime $\tau_{1D} = 110$ ps provides a 1D-exciton-wavefunction value of $|\varphi(0)|^{-2} = 20$ nm via equation (1). Note that $|\varphi(0)|^{-2}$ represents the 1D exciton size and indicates the probability of finding an electron and a hole at the same position in a 1D exciton. The obtained results, together with the exciton binding energy $E_B = 14$ meV measured for the present T-wires, can be compared with model calculations. Indeed, the value $|\varphi(0)|^{-2} = 15\text{--}16$ nm ($\tau_{1D} = 80$ ps) calculated based on simple 1D models^{27–30} is close to the result obtained in this study. It should also be noted that the obtained 1D exciton size of 20 nm along the wire is not very different from the 2D exciton diameters of 10–20 nm in GaAs wells. This establishes that the longer (by one order of magnitude) intrinsic radiative lifetime of 1D excitons compared with that of 2D excitons cannot be attributed to the internal motion of 1D excitons but alternatively to their center-of-mass motion with lateral confinement, as mentioned in the introduction.

The evaluation of the absorption cross section was performed with such an approximation that radiative coupling effects caused by the dipole-dipole interactions between the arrayed T-wires are ignorable small. This approximation is justified because of a high background dielectric constant of GaAs of around 3.6, a large bulk exciton Bohr radius of about 15 nm, and a small bulk longitudinal-transverse splitting of about 0.1 meV. Indeed, a theoretical calculation³¹ has shown that the effect of dipole-dipole coupling for the case of GaAs QWs separated by 20 nm is very tiny and not measurable in absorption spectra or in time-resolved PL. Our present T-wires are separated by 42 nm and the wire volume is far smaller than QWs. Therefore, the effect of dipole-dipole coupling should be even smaller.

Our proposed method of 1D-exciton intrinsic radiative-lifetime measurement via absorbance and the relevant universal relationships between the Einstein's A–B coefficients of 1D exciton are applicable to nano-tubes^{6–10}, nano-wires^{32–34} and nano-columns/needles^{35,36} comprised of various materials, and are useful in establishing intriguing 1D exciton physics.

Methods

The sample was fabricated by cleaved-edged over-growth and interrupted annealing using molecular beam epitaxy. The fabrication method is very similar to that used to produce other T-wire structures reported previously and is illustrated in detail in the supplementary information. The sample was grown as follows: During the first MBE growth step on the GaAs (001) substrate, a GaAs buffer layer, a 1- μm $\text{Al}_{0.5}\text{Ga}_{0.5}\text{As}$ bottom carrier-blocking layer, 100 periods of $\text{Al}_{0.08}\text{Ga}_{0.92}\text{As}/\text{Al}_{0.34}\text{Ga}_{0.66}\text{As}$ stem multiple quantum wells with well and barrier thicknesses of 14.15 and 41.88 nm, respectively, a 1- μm $\text{Al}_{0.5}\text{Ga}_{0.5}\text{As}$ top carrier-blocking layer, and a 3- μm GaAs cap layer were grown at a growth temperature of 620°C. After in situ cleavage of the sample, a second MBE growth step was performed at a substrate temperature of 490°C on the fresh (110) surface exposed by the cleavage. In the second growth step, a 6-nm arm quantum well, a 10-nm $\text{Al}_{0.5}\text{Ga}_{0.5}\text{As}$ barrier layer, and 175-nm $\text{Al}_{0.12}\text{Ga}_{0.88}\text{As}$ and 960-nm $\text{Al}_{0.5}\text{Ga}_{0.5}\text{As}$ cladding layers were grown. To improve the interface quality of the arm quantum well, 10-minute growth-interrupt annealing was performed at an elevated substrate temperature of 650°C after the growth of the arm well.

For optical measurements, the samples were set in a custom-built cryostat cooled by flowing liquid helium. A heater was set in the cryostat such that the sample temperature could be varied from 4 K to room temperature. The quality and uniformity of the wires were verified by conducting a micro-PL scan, and the best sample was chosen for study. The micro-PL and micro-PL scans were performed using a continuous-wave titanium-sapphire (TiS) laser (the wavelength was continuously tuned from 700 to 850 nm in ~ 0.1 nm steps) and a spectrometer equipped with a liquid-nitrogen-cooled silicon charge-coupled device (CCD). The excitation light from the TiS laser was incident on the central T-wire region with a spot size of approximately 1 μm perpendicularly to the arm well and a polarization parallel to the T-wires (z direction), and PL polarized perpendicularly to the T-wires was detected in the backward scattering geometry. The PLE spectrum was obtained by measuring the integrated intensity of the entire T-wire PL while scanning the excitation photon

energy. The temperature-dependent time-resolved PL of 1D excitons was measured in the T-wires between 5 and 100 K via the time-correlated single-photon counting method using a mode-locked TiS laser with a pulse duration of 2 ps and a repetition rate of 80 MHz. All measurements were performed under low-density excitation conditions to prevent the formation of biexcitons or electron-hole plasmas.

1. Andreani, L. C., Tassone, F. & Bassani, F. Radiative lifetime of free excitons in quantum wells. *Solid State Communications* **77**, 641–645 (1991).
2. Citrin, D. S. Long intrinsic radiative lifetimes of excitons in quantum wires. *Phys. Rev. Lett.* **69**, 3393–3396 (1992).
3. Akiyama, H. *et al.* Thermalization effect on radiative decay of exciton in quantum wire. *Phys. Rev. Lett.* **72**, 924–927 (1994).
4. Gershoni, D. *et al.* Radiative lifetimes of excitons in quantum wires. *Phys. Rev. B* **50**, 8930–8933 (1994).
5. Oberli, D. Y., Dupertuis, M. A., Reinhardt, F. & Kapon, E. Effect of disorder on the temperature dependence of radiative lifetimes in V-groove quantum wires. *Phys. Rev. B* **59**, 2910–2914 (1999).
6. Spataru, C. D. *et al.* Theory and ab Initio calculation of radiative lifetime of excitons in semiconducting carbon nanotubes. *Phys. Rev. Lett.* **95**, 247402 (2005).
7. Wang, F. *et al.* Time-resolved fluorescence of carbon nanotubes and its implication for radiative lifetimes. *Phys. Rev. Lett.* **92**, 177401 (2004).
8. Perebeinos, V., Tersoff, J. & Avouris, P. Radiative lifetime of excitons in carbon nanotubes. *Nano Lett.* **5**, 2495–2499 (2005).
9. Scholes, G. D. & Rumbles, G. Excitons in nanoscale systems. *Nature material* **5**, 683–696 (2006).
10. Miyauchi, Y., Hirori, H., Matsuda, K. & Kanemitsu, Y. Radiative lifetimes and coherence lengths of one-dimensional excitons in single-walled carbon nanotubes. *Phys. Rev. B* **80**, 081410(R) (2009).
11. Citrin, D. S. Exciton radiative decay and polaritons in multi-quantum wells: quantum-well-to-superlattice crossover. *Solid State Commun.* **89**, 139–143 (1994).
12. Feldmann, J. *et al.* Linewidth dependence of radiative exciton lifetimes in quantum wells. *Phys. Rev. Lett.* **59**, 2337–2340 (1987).
13. Stobbe, S. *et al.* Frequency dependence of the radiative decay rate of excitons in self-assembled quantum dots: Experiment and theory. *Phys. Rev. B* **80**, 155307 (2009).
14. Yoshita, M. *et al.* Quantitative absorption spectra of quantum wires measured by analysis of attenuated internal emissions. *Appl. Phys. Lett.* **100**, 112101 (2012).
15. Takahashi, Y. *et al.* Strong photoabsorption by a single-quantum wire in waveguide-transmission spectroscopy. *Appl. Phys. Lett.* **86**, 243101 (2005).
16. Hayamizu, Y. *et al.* Biexciton Gain and the Mott Transition in GaAs Quantum Wires. *Phys. Rev. Lett.* **99**, 167403 (2007).
17. Yoshita, M. *et al.* Applicability of continuum absorption in semiconductor quantum wells to absolute absorption-strength standards. *Appl. Phys. Lett.* **101**, 032108 (2012).
18. Liu, H. P. *et al.* Large-scale single-chirality separation of single-wall carbon nanotubes by simple gel chromatography. *Nature Communications* **2**, 309 (2011).
19. Liu, H. P. *et al.* Diameter-selective metal/semiconductor separation of single-wall carbon nanotubes by agarose gel. *J. Phys. Chem. C* **114**(20), 9270–9276 (2010).
20. Chang, Y. C., Chang, L. L. & Esaki, L. A new one-dimensional quantum well structure. *Appl. Phys. Lett.* **47**, 1324 (1985).
21. Wegscheider, W. *et al.* Lasing from excitons in quantum wires. *Phys. Rev. Lett.* **71**, 4071 (1993).
22. Klitzing, K. V., Dorda, G. & Pepper, M. New method for high-accuracy determination of the fine-structure constant based on quantized hall resistance. *Phys. Rev. Lett.* **45**, 494–497 (1980).
23. Ando, T., Zheng, Y. & Suzuura, H. Dynamical conductivity and zero-mode anomaly in honeycomb lattices. *J. Phys. Soc. Jpn.* **71**, 1318–1324 (2002).
24. Stauber, T., Peres, N. M. R. & Geim, A. K. Optical conductivity of graphene in the visible region of the spectrum. *Phys. Rev. B* **78**, 085432 (2008).
25. Davies John, H. *The physics of low dimensional semiconductors: an introduction.* Cambridge University Press, 1997.
26. Masumoto, Y., Matsuura, M., Tarucha, S. & Okamoto, H. Direct experimental observation of two-dimensional shrinkage of the exciton wave function in quantum wells. *Phys. Rev. B* **32**, 4275–4278 (1985).
27. Loudon, R. One-dimensional hydrogen atom. *Am. J. Phys.* **27**, 649–655 (1959).
28. Ogawa, T. & Takagahara, T. Optical absorption and Sommerfeld factors of one-dimensional semiconductors: An exact treatment of excitonic effects. *Phys. Rev. B* **44**, 8138–8156 (1991).
29. Szymanska, M. H., Littlewood, P. B. & Needs, R. J. Excitons in T-shaped quantum wires. *Phys. Rev. B* **63**, 205317 (2001).
30. Benner, S. & Haug, H. Plasma-density dependence of the optical spectra for quasi-one-dimensional quantum well wires. *Europhys. Lett.* **16**, 579 (1991).
31. Batsch, M. *et al.* Dipole-dipole coupling of excitons in double quantum wells. *Phys. Rev. B* **48**, 11817–11826 (1993).
32. Duan, X., Huang, Y., Cui, Y., Wang, J. & Lieber, C. M. Indium phosphide nanowires as building blocks for nanoscale electronic and optoelectronic devices. *Nature* **409**, 66–69 (2001).
33. Yan, R., Gargas, D. & Yang, P. Nanowire Photonics. *Nature Photonics* **3**, 569–576 (2009).



34. Yang, C., Barrelet, C. J., Capasso, F. & Lieber, C. M. Single p-type/intrinsic/n-type silicon nanowires as nanoscale avalanche photodetectors. *Nano Letters* **6**, 2929–2934 (2006).
35. Chen, R. *et al.* Nanolasers grown on silicon. *Nature Photonics* **5**, 170–175 (2011).
36. Kikuchi, A., Kawai, M., Tada, M. & Kishino, K. InGaN/GaN multiple quantum disk nanocolumn light-emitting diodes grown on (111) Si substrate. *Jpn. J. Appl. Phys.* **43**, L1524–L1526 (2004).

Acknowledgements

This work was partially supported by KAKENHI (nos. 20104004 and 23104715) for the DYCE research area from the MEXT, Japan. The work at Princeton was partially funded by the Gordon and Betty Moore Foundation and the National Science Foundation MRSEC program through the Princeton Center for Complex Materials (DMR-0819860). A. I. is grateful for the support of the Program to Disseminate Tenure Tracking System of the MEXT, Japan.

Author contributions

H.A., M.Y. and S.C. conceived the project. L.N.P. and K.W.W. fabricated the sample. S.C., M.Y. and S.M. performed the temperature-dependent time-resolved PL measurements. S.C., S.M. and T.M. performed the micro-PL measurements and extracted the PLE spectra. S.C., M.Y. and H.A. calibrated the absorption rate in the PLE spectra. A.I., M.Y., H.A. and S.C. performed the theoretical derivation. S.C., M.Y., H.A. and H.Y. analyzed the results and wrote the paper.

Additional information

Supplementary information accompanies this paper at <http://www.nature.com/scientificreports>

Competing financial interests: The authors declare no competing financial interests.

License: This work is licensed under a Creative Commons Attribution-NonCommercial-ShareAlike 3.0 Unported License. To view a copy of this license, visit <http://creativecommons.org/licenses/by-nc-sa/3.0/>

How to cite this article: Chen, S. *et al.* Intrinsic radiative lifetime derived via absorption cross section of one-dimensional excitons. *Sci. Rep.* **3**, 1941; DOI:10.1038/srep01941 (2013).